




Spatial coherence effects of stochastic optical beams in periodic potentials

M. J. Cirino ^{*}, P. A. Brandão [†] and S. B. Cavalcanti [‡]

Universidade Federal de Alagoas, Instituto de Física, 57072-900, Brazil



(Received 30 November 2022; accepted 10 March 2023; published 23 March 2023)

The interaction between a partially coherent field with a one-dimensional periodic photonic environment is investigated within the framework of Floquet-Bloch modes. To this end, we describe the interplay between lattice properties and field fluctuations by considering the optical beam as a linear combination of Floquet-Bloch modes, whose coefficients are described by a stationary random process. It is demonstrated that the propagation of partially coherent beams depends not only on the average of the excitation of each band but also on the correlations existent among the various bands supported by the lattice.

DOI: [10.1103/PhysRevA.107.033518](https://doi.org/10.1103/PhysRevA.107.033518)

I. INTRODUCTION

Wave propagation through periodic structures has been extensively studied in diverse physical environments such as optical lattices, waveguide arrays, and Bose-Einstein condensates, among others. Stemming from the analogy between electromagnetic waves in a periodic dielectric structure and electrons in a periodic atomic potential, work based on Floquet-Bloch (FB) optical modes has flourished since the advent of photonic crystals [1–4]. One of the most important features exhibited by wave propagation in periodic media is the existence of bands and forbidden frequency gaps for electromagnetic waves, [5,6]. Their existence in the photonic density of states is of fundamental importance as dispersion and diffraction are strongly enhanced, modifying severely the properties of light propagation. Based on these facts, theoretical and experimental research on modulated photonic lattices has been developed intensely in the last decades, revealing rich phenomena [2,7].

However, in real experiments all light sources fluctuate in the sense that the fields they generate undergo random fluctuations, and it is well known that the spatial coherence properties of a source strongly affect the spectrum of the propagating wave. By coherence here we mean a measure of correlations between the components of the fluctuating field at two or more points in the space at the same time. Coherence is a fundamental concept about the nature of light and investigating its influence upon optical systems is necessary if one is to achieve spatial coherence control, as it is required in many practical applications such as imaging [8], tomography [9], and beam propagation [10], among many others [11,12]. Therefore, owing to the fact that fluctuations are always present in real systems, one must include them in the investigation of periodic systems to find the extent that they might modify the spectrum dynamics [13]. To this

end, one may rely on the techniques of statistical optics, also known as optical coherence theory [14,15].

Based on the above discussion, in this paper we introduce a method to understand the interaction between a partially coherent field with a one-dimensional periodic photonic environment within the framework of Floquet-Bloch modes together with a space-frequency representation of stationary random processes. For comparison purposes, we apply our scheme to the propagation of a deterministic Gaussian beam as well as the propagation of partially coherent Gaussian-Schell beams [16]. We choose to work with the FB basis considering that a FB wave traveling through a periodic medium is the counterpart of a plane wave traveling through a homogeneous medium. A FB mode itself is composed of a group of plane waves. In both cases the final beam is defined as the linear combination of the FB modes, which are the eigenvalues of the paraxial equation. In the partially coherent case, each linear combination is just a member of an ensemble of possible output beam shapes. The output beam profiles are determined by the interference among multi FB modes. We shall describe the role played by band correlations and their consequences. To this end, in the next section we introduce our theory in the case of a deterministic beam and apply it to a wide Gaussian beam. In Sec. III we present the generalization of the deterministic theory to include the statistical properties of the incident beam, and describe the evolution of the Gaussian-Schell beam. In Sec. IV we conclude.

II. DETERMINISTIC THEORY

Let us begin by considering a monochromatic realization of an optical field represented by the slowly varying envelope $\psi(x, z)$ propagating along the homogeneous z direction through a periodic medium positioned along the transverse direction x . Its dynamical behavior can be well described by the normalized paraxial wave equation

$$i \frac{\partial \psi(x, z)}{\partial z} + \frac{\partial^2 \psi(x, z)}{\partial x^2} + V(x) \psi(x, z) = 0, \quad (1)$$

^{*}miqueias@fis.ufal.br

[†]paulo.brandao@fis.ufal.br

[‡]solange@fis.ufal.br

where $\psi(x, z)$ represents the normalized electric field envelope. The function $V(x+a) = V(x)$ describes the periodic lattice and is proportional to the refractive index of the material. We suppose that it has the following general form:

$$V(x) = \sum_{m=-\infty}^{\infty} V_m e^{2\pi imx/a}, \quad (2)$$

where the parameter a is a positive number representing the lattice period and V_m represents the m th Fourier amplitude, which is a complex number, in general.

The eigenstates of the paraxial wave equation are defined as $\psi_n(x, k) = u_n(x, k)e^{i\beta_n(k)z}$, with k as the Bloch wave number corresponding to the FB mode $u_n(x, k)$, which satisfies the following equation:

$$\frac{d^2 u_n(x, k)}{dx^2} + V(x)u_n(x, k) = \beta_n(k)u_n(x, k); \quad (3)$$

here, we fix the Bloch wave number within the first Brillouin Zone (BZ), that is $k \in [-\pi/a, \pi/a]$; n is the band index; and $\beta_n(k)$ is the propagation constant of the FB wave. The FB modes are the eigenstates of the paraxial wave equation (3). In a periodic medium they play the same role as plane waves in a homogeneous medium. They are stationary states just like in the solid state, except that here in the space description they are diffractionless solutions, meaning that the intensity is independent of the propagation direction. These modes are fully determined by the structure of the lattice and remain dormant unless they become excited by the incident wave field. In a linear propagation regime, each FB mode acquires its own phase, independent of the other modes. Since these modes remain the same in spite of the different relative phases acquired during propagation, the beam may have a completely different profile at the output compared to the input profile according to the dynamics determined by the band structure, as we shall demonstrate in the following.

We begin by considering that a general solution for Eq. (1) can be written as a linear superposition of FB modes, in the sense that each mode supported by the lattice is a FB wave with its own propagation constant β_n :

$$\psi(x, z) = \sum_{n=1}^{\infty} \int_{-\pi/a}^{\pi/a} c_n(k) u_n(x, k) e^{i\beta_n(k)z} dk, \quad (4)$$

where $c_n(k)$ is the participation coefficient of band n at wave vector k . It represents the relative power within the correspondent FB mode with Bloch wave number k and band n . The envelope profile of the optical field is then determined by the interference among these modes. These coefficients are fully defined at the input plane $z = 0$, and can be calculated from

$$c_n(k) = \int_{-\infty}^{\infty} u_n^*(x, k) \psi(x, 0) dx, \quad (5)$$

after the orthogonality between FB modes $\int_{-\infty}^{\infty} u_n^*(x, k_1) u_m(x, k_2) dx = \delta_{nm} \delta(k_1 - k_2)$ was used, and $\psi(x, 0)$ describes the beam profile at $z = 0$. Depending on the variation of the beam amplitude at $z = 0$, and also on the values of the Fourier components V_m , the incident beam may excite FB modes belonging to more than one band.

Figure 1 displays the first three bands for a periodic lattice represented by the truncated expansion of Eq. (2), that is,

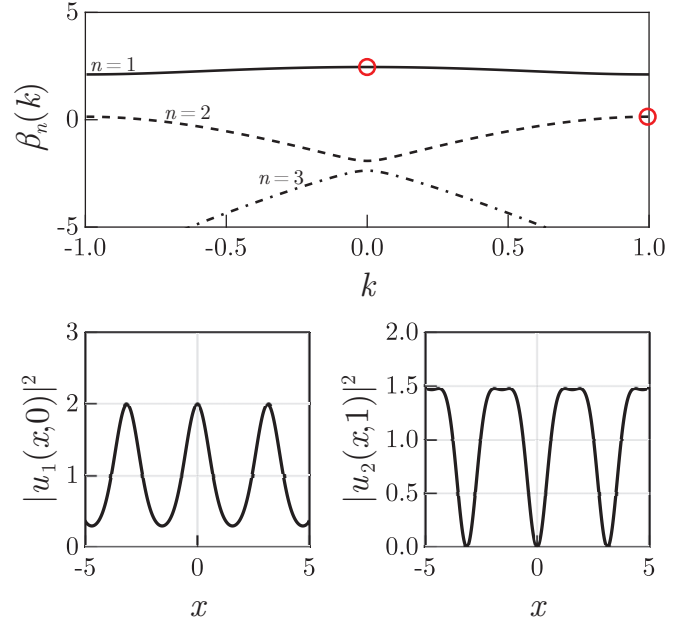


FIG. 1. (Top) Propagation constant $\beta_n(k)$ versus Bloch wave number k for modes $n = 1, 2$, and 3 and fixed potential amplitude $A = 4$. Floquet-Bloch mode amplitudes $|u_1(x, k = 0)|^2$ (bottom left) and $|u_2(x, k = 1)|^2$ (bottom right) versus lattice position x . The red circles in the top panel represent the propagation numbers for each of the FB modes represented in the bottom panels.

$V(x) = A \cos^2 x$, which is the potential used in all subsequent analysis. More specifically, $V_0 = A/2$ and $V_{\pm 1} = A/4$ and $V_m = 0$ otherwise. Along with the bands, the figure displays two FB modes corresponding to Bloch wave number $k = 0$ (bottom left) and $k = 1$ (bottom right) for $n = 1$ and $n = 2$, respectively. The zeros of FB modes at the band edges are characteristic of Hermitian lattices only [17].

Gaussian beam source

Let us now apply the formalism developed above by considering the propagation of a fully coherent Gaussian beam described by the incident field amplitude,

$$\psi(x, 0) = S_0 e^{-x^2/2\sigma^2} e^{iqx}, \quad (6)$$

where σ is the beam width, q the transverse momentum k , and S_0 the field amplitude, at $x = 0$. To gain physical insight into the contribution of the Bloch coefficients $c_n(k)$, we write the Bloch mode $u_n(x, k)$ as

$$u_n(x, k) = e^{ikx} \sum_{\alpha=-\infty}^{\infty} d_{\alpha}^{(n)}(k) e^{2\pi i \alpha x/a}, \quad (7)$$

where $d_{\alpha}^{(n)}(k)$ is the α th expansion coefficient of band n and Bloch wave number k . Next, we substitute (6) and (7) into (5) to obtain

$$c_n(k) = \sigma S_0 \sqrt{2\pi} \sum_{\alpha=-\infty}^{\infty} [d_{\alpha}^{(n)}(k)]^* e^{-(\sigma^2/2)(2\pi\alpha/a+k-q)^2}. \quad (8)$$

Since $d_{\alpha}^{(n)}(k)$ (for varying α) are the eigenvectors' coefficients of the matrix obtained after substituting (7) into (3),

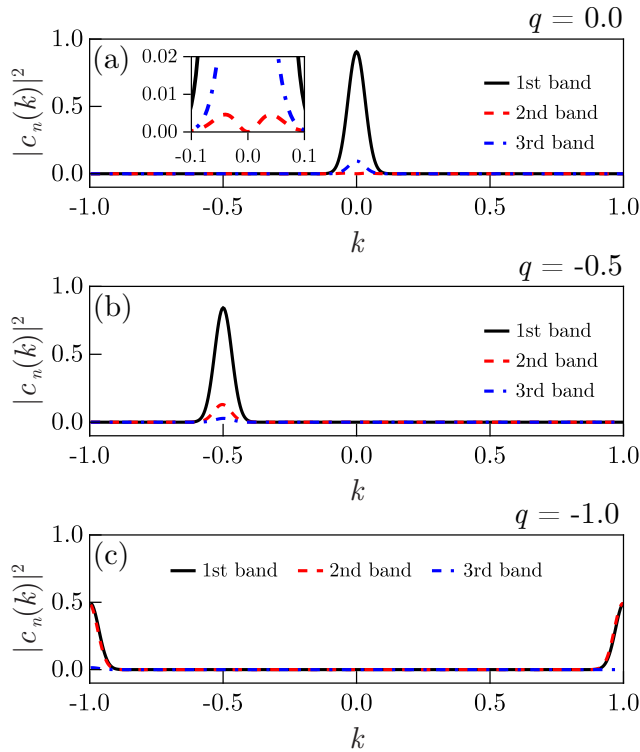


FIG. 2. Absolute squared Floquet-Bloch coefficients $|c_n(k)|^2$ versus wave number k , for fixed $A = 4.0$ input beam width $\sigma = 7\pi$ and various input wave numbers: (a) $q = 0.0$ (the inset illustrates the contribution of the second and third bands), (b) $q = -0.5$, and (c) $q = -1.0$.

Eq. (8) is more suitable from a computational point of view since one does not need to deal with the integration over the x axis, as Eq. (5) suggests. Also, for a fixed Bloch wave vector k and moderate values of A , only a few of $d_\alpha^{(n)}(k)$ are significantly different from zero, as we show in the examples discussed below. Figure 2 illustrates the participation coefficients $|c_n(k)|^2$ (normalized by $\sigma S_0 \sqrt{2\pi}$) for the first three bands $n = 1, 2, 3$. Figure 2(a) displays the coefficient profiles for $q = 0$ (normal incidence) and indicates that most of the contribution comes from the first band, with a small fraction of the third band, and as illustrated in the inset an even smaller contribution of the second band. Part (b) is plotted for $q = -0.5$ and shows a similar behavior, with the first band exhibiting most of the contribution, but now the second band contribution grows and overcomes the contribution of the third one.

By simply changing the excitation angle, which determines the transverse momentum q of a beam, one can dynamically control its diffraction properties [18]. We turn to Fig. 2(c), the case $q = -1$, corresponding to Bragg scattering. We see that the first two bands exhibit identical contributions to the overall beam evolution. Since the beam direction is determined essentially by the direction of the group velocity $\nabla_k \beta_n(k)$, which is perpendicular to the transmission band, it is expected that in the Bragg condition the beam evolves mainly along the z direction, diffractionless as shown in Fig. 1. This claim is confirmed by Fig. 3(a), which displays the plot of $|\psi(x, z)|^2$, calculated directly from (4).

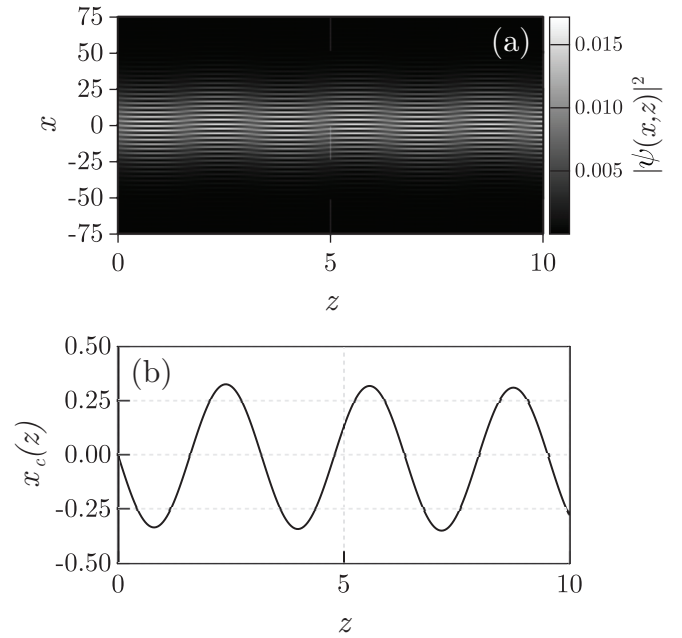


FIG. 3. (a) Beam intensity $|\psi(x, z)|^2$. (b) Beam center oscillation $x_c(z)$ versus propagation distance z for input wave number $q = -1.0$, input beam width $\sigma = 7\pi$, and potential amplitude $A = 4.0$.

After a close inspection of Fig. 3(a), one finds that the beam center oscillates during propagation along z . Let us then define the beam center as

$$x_c(z) = \frac{\int x |\psi(x, z)|^2 dx}{\int |\psi(x, z)|^2 dx}. \quad (9)$$

Figure 3(b) displays the beam center oscillations $x_c(z)$. It should be pointed out that these oscillations are not centered around $x_c = 0$. There is a slow rectilinear movement in the negative x direction superposing the oscillations. This behavior resembles the quivering of the free Dirac electron, well known by Zitterbewegung (ZB) [19]. In the context of photonic systems such oscillations have been reported in the case of waveguide arrays [20–22].

III. STOCHASTIC THEORY

Random fluctuations are inherent in all optical fields irrespective of their origin; whether spontaneous emission, temperature fluctuations, or mechanical vibrations, among many others, the fluctuations are always present. Therefore, to deal with measurable quantities in optical systems one must incorporate statistical concepts to the theory to characterize, not the field evolution in one space-time point, but the correlations between two (or more) space-time points. In second-order classical statistical optics, one characterizes the two-point correlations by using the cross-spectral density function. Under general conditions, likely to be valid in many systems of interest, the cross-spectral density of a statistical stationary source is defined as

$$W(x_1, x_2, z) = \langle \psi^*(x_1, z) \psi(x_2, z) \rangle_\omega, \quad (10)$$

where $\langle \cdot \rangle_\omega$ implies an ensemble average of monochromatic realizations of the incident optical field.

A random beam can be generated by choosing the FB functions as an orthonormal basis to obtain a linear combination that represents the beam profile inside the periodic medium, as suggested in the last section. However, now we suppose that the respective FB coefficients $c_n(k)$ are described by stationary random processes of the FB wave number so that each mode represents one configuration of the ensemble. The evolution of the overall field $\psi(x, z)$ depends not only on the average values of $c_n(k)$ but also on the correlations existent between the bands that correspond to the cross-correlations $C_{mn}(k_1, k_2) = \langle c_m^*(k_1)c_n(k_2) \rangle_\omega$. In this way, one may speak of the correlations between $c_m(k_1)$ and $c_n(k_2)$ and study their influence upon the evolution of a partially coherent beam. Previous works on the propagation of partially coherent beams in periodic structures have been published in nonlinear [23] and linear [24,25] systems. The approach taken by Hoenders and Bertolotti is very similar to ours, differing in that they assume a weakly periodic media and a nonparaxial propagation, which results in a somewhat more involved analysis of the propagation dynamics.

Thus, in the following we shall be concerned with this problem: given the initial distribution of field correlations $W(x_1, x_2, 0)$, how can one obtain the cross-spectral density at a given $z > 0$? The answer to this question lies within the correlation $C_{mn}(k_1, k_2)$ between $c_n(k_1)$ and $c_m(k_2)$ that can be directly evaluated from (5):

$$\begin{aligned} C_{mn}(k_1, k_2) &= \langle c_m^*(k_1)c_n(k_2) \rangle_\omega \\ &= \iint u_m(x_1, k_1)u_n^*(x_2, k_2)W(x_1, x_2, 0)dx_1dx_2. \end{aligned} \quad (11)$$

The coefficients $C_{mn}(k_1, k_2)$ represent a measure of the correlations between bands m and n for FB wave numbers k_1 and k_2 . Once the coefficients $C_{mn}(k_1, k_2)$ are obtained, and with the knowledge of the statistical properties at the input, the cross-spectral density $W(x_1, x_2, z)$ for $z > 0$ is readily obtained for any state of light:

$$\begin{aligned} W(x_1, x_2, z) &= \sum_{n,m=1}^{\infty} \int_{-\pi/a}^{\pi/a} dk_1 \int_{-\pi/a}^{\pi/a} dk_2 \\ &\times C_{mn}(k_1, k_2)u_m^*(x_1, k_1)u_n(x_2, k_2) \\ &\times e^{-i[\beta_m(k_1) - \beta_n(k_2)]z}. \end{aligned} \quad (12)$$

The averaged intensity is given by $S(x, z) = W(x, x, z) = \langle |\psi(x, z)|^2 \rangle$, that is,

$$\begin{aligned} S(x, z) &= \sum_{n,m=1}^{\infty} \int_{-\pi/a}^{\pi/a} dk_1 \int_{-\pi/a}^{\pi/a} dk_2 \\ &\times C_{mn}(k_1, k_2)u_m^*(x, k_1)u_n(x, k_2) \\ &\times e^{-i[\beta_m(k_1) - \beta_n(k_2)]z}. \end{aligned} \quad (13)$$

By inspection of Eq. (13), one can conclude that the spatial correlation represented by the cross-spectral function $W(x_1, x_2, z)$ does induce additional FB modes to the overall field. One may visualize the correlations through the spectral degree of coherence, a convenient quantity that measures the normalized degree of coherence between the modes, defined

here as

$$\mu_{nm}(k_1, k_2) = \frac{\langle c_n^*(k_1)c_m(k_2) \rangle}{\sqrt{\langle |c_n(k_1)|^2 \rangle \langle |c_m(k_2)|^2 \rangle}}, \quad (14)$$

which satisfies the condition $0 \leq |\mu_{nm}(k_1, k_2)| \leq 1$. When $|\mu_{nm}(k_1, k_2)| = 1$, the field is fully correlated at wave numbers (k_1, k_2) and bands (n, m) . In the opposite extreme, the field is fully uncorrelated, and in between these two extreme cases, the field is partially coherent. Next, we illustrate this theory, applying it to the specific case of Gaussian-Schell sources.

Gaussian-Schell sources

Gaussian-Schell models describe an important class of partially coherent beams that are easily created in the laboratory [26,27]. They are characterized by a spectral degree of coherence that depends only on the difference between the location of the two points, x_1 and x_2 . Considering that the field fluctuations are well described by a stationary process, one suitable model for the cross-spectral density function for this class of beams at the input is given by

$$W(x_1, x_2, 0) = S_0^2 e^{-(x_1^2+x_2^2)/2\sigma^2} e^{-(x_1-x_2)^2/2\delta^2} e^{-iq(x_1-x_2)}, \quad (15)$$

where S_0 is the field amplitude, σ is the beam width, δ is the coherence parameter ($\delta \rightarrow \infty$ describing a fully spatially coherent beam), and $-q(x_1 - x_2)$ is a phase factor related to the transverse incident wave vector q .

The FB correlation coefficients $C_{mn}(k_1, k_2)$ are written in the same form as in Eq. (8) after substituting (15) and (7) into (11) to obtain

$$\begin{aligned} C_{mn}(k_1, k_2) &= \frac{2\pi S_0^2 \delta \sigma^2}{\sqrt{\delta^2 + 2\sigma^2}} \sum_{\alpha, \beta=-\infty}^{\infty} d_\alpha^{(m)}(k_1) [d_\beta^{(n)}(k_2)]^* \\ &\times \exp \left[-\frac{\delta^2 \sigma^2 (k_1 + \frac{2\pi}{a} \alpha - q)^2}{2(\delta^2 + 2\sigma^2)} \right] \\ &\times \exp \left[-\frac{\delta^2 \sigma^2 (k_2 + \frac{2\pi}{a} \beta - q)^2}{2(\delta^2 + 2\sigma^2)} \right] \\ &\times \exp \left\{ -\frac{\sigma^4 [k_1 - k_2 + \frac{2\pi}{a} (\alpha - \beta)]^2}{2(\delta^2 + 2\sigma^2)} \right\}. \end{aligned} \quad (16)$$

Equation (16) is a generalization of the absolute square of Eq. (8). Note that by taking the limit $\delta \rightarrow \infty$, with $k_1 = k_2 = k$ and $m = n$, one retrieves Eq. (8). It is easy to see that in the special case of high coherence, $\delta \rightarrow \infty$, the coefficients $C_{mn}(k_1, k_2)$ can be written as a product between two independent functions of n (m) and k_1 (k_2), which is indicative of a full correlation between the modes. Figure 4 illustrates the mean participation coefficients $\langle |c_n(k)|^2 \rangle$ for two FB bands ($n = 1$ and 2), for several values of the coherence parameter δ , and for three incidence wave vectors $q = 0$, $q = -0.5$ and $q = -1.0$ where all the coefficients are divided by the constant factor multiplying the summation. The arrow in Fig. 4(a) indicates the growth direction of the coherence parameter, and this applies to all plots in the figure. It is clear that as the spatial coherence decreases, the contribution to the overall beam increases in the sense that many FB modes are now excited when compared to the fully coherent case. Conversely,

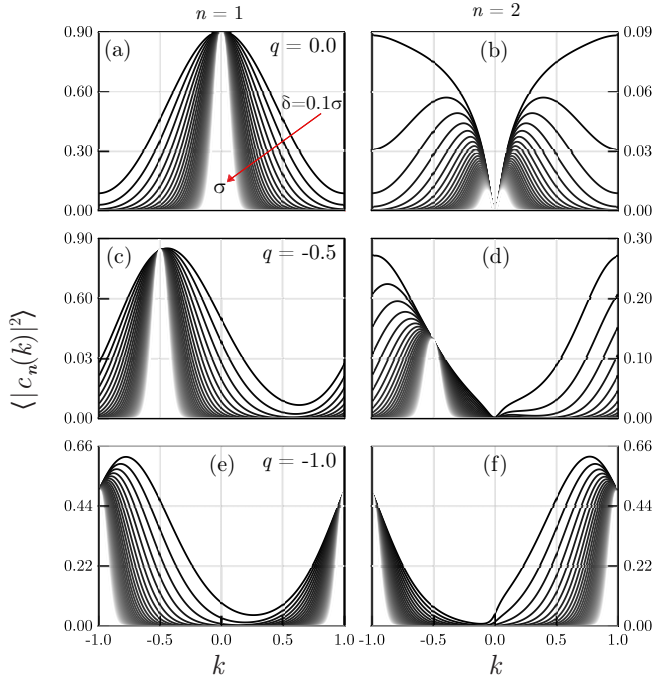


FIG. 4. Mean absolute squared of the first two FB coefficients $\langle |c_n(k)|^2 \rangle$ versus wave number k with input beam width $\sigma = 7\pi$, amplitude $A = 4.0$, and coherence parameter $\delta \in [\sigma/10, \sigma]$ for various input wave numbers: (a and b) with $q = 0.0$; (c and d) with $q = -0.5$; and (e and f) with $q = -1.0$. The arrow indicates increasing δ . The n th column corresponds to the n th mode, $n = 1, 2$.

as the spatial coherence increases, the broadening that once occupied the whole Brillouin zone becomes smaller and tends to localize along a limited band around $k = 0$, as in the fully coherent case depicted in Fig. 2. Therefore, it is clear that the lack of spatial coherence does indeed excite additional FB modes, broadening the spectrum. The extent of the broadening can be controlled by the coherence degree, a feature that is quite interesting from the point of view of applications.

The spectral degree of coherence $\mu_{nm}(k_1, k_2)$ as a function of the coherence parameter δ is displayed in Fig. 5 for some FB wave numbers k_1 and k_2 in the Brillouin zone, where we considered the correlations between the first and second bands $n = 1$ and $n = 2$. Figures 5(a) and 5(d) show an example at the same FB wave number, k . In the solid state, a transition between bands at the same k value is considered a direct transition. Otherwise, it is known as indirect. Here, we adapt this nomenclature referring to direct points $k_1 = k_2$ and indirect ones $k_1 \neq k_2$. Therefore, Figs. 5(a) and 5(d) are direct points, while Figs. 5(b) and 5(c) are indirect points. In both cases, direct or indirect, as the coherence parameter δ increases, the correlation between bands also increases, reaching the unit value asymptotically $\mu_{12} \rightarrow 1$ as $\delta \rightarrow \infty$ as expected. However, for indirect points the rate at which the coherence degree increases is much slower than the rate for direct points.

The resulting beam spectral density is plotted in Fig. 6(a) against the propagation distance z for $\delta = 0.01\sigma$. As expected, in this low-coherence regime, the influence of the coherence parameter upon the propagation causes spreading of the beam

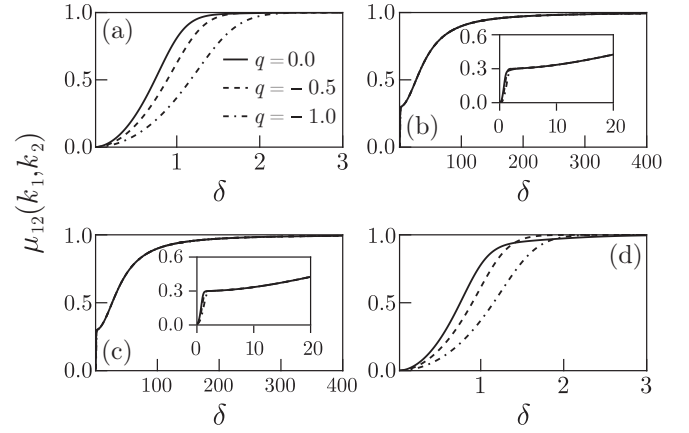


FIG. 5. Spectral degree of coherence $\mu_{12}(k_1, k_2)$ versus the coherence parameter δ for input beam width $\sigma = 7\pi$ and amplitude $A = 4.0$ at various incident angles, correspondent to $q = -1.0$ (solid line), $q = -0.5$ (dashed line), and $q = 0.0$ (dot-dashed line). Several spectral degrees of coherence between points of the Brillouin zone are displayed: (a) $k_1 = k_2 = -0.3$; (b) $k_1 = -0.2$ and $k_2 = -0.3$; (c) $k_2 = -0.3$ and $k_1 = -0.2$; and (d) $k_1 = k_2 = -0.2$.

intensity all over the BZ, resembling the case where there is no periodic lattice at all, as illustrated.

Now we turn to Fig. 6(b), where the beam center $X_c(z)$ is depicted according to the definition

$$X_c(z) = \frac{\int x S(x, z) dx}{\int S(x, z) dx}. \quad (17)$$

It can be demonstrated that Eq. (17) has the general form $X_c(z) = X_c(0) + vz + p(z)$, where $p(z)$ is a periodic

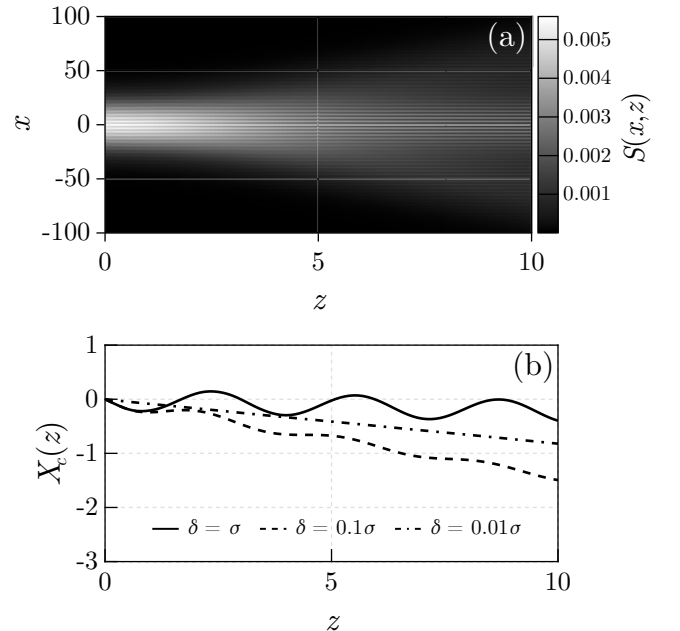


FIG. 6. (a) Beam spectral density $S(x, z)$ with coherence parameter $\delta = \sigma/100$. (b) Mean beam center oscillation $X_c(z)$ versus propagation distance z for three coherence parameters: σ , $\sigma/10$, and $\sigma/100$. For input wave number $q = -1.0$, input beam width $\sigma = 7\pi$ and potential amplitude $A = 4.0$.

function of z that depends on the correlation between bands $\langle c_n^*(k)c_m(k) \rangle$ and v denotes the linear ramp which depends on the average values $\langle |c_n(k)|^2 \rangle$ for each band n . They both also depend on the group velocity $d\beta_n(k)/dk$. The exact dependence of $X_c(z)$ on the cross-correlations $C_{mn}(k_1, k_2)$ and the group velocity $d\beta_n(k)/dk$ is so intricate that it will be investigated in more detail in a future work. Nevertheless, one finds that for an intermediate regime ($\delta = 0.1\sigma$), although the oscillations executed by the beam center undergo damping, they do not cease to exist. However, as δ decreases, the damping effect is more severe and tends to wipe them off to the extent that only the rectilinear movement is left. This is expected to occur in view of the previous discussion involving the direction of the group velocity of a Gaussian wave packet, which is determined by the band diagram illustrated at the top of Fig. 1 and by the distribution of the absolute squared Floquet-Bloch coefficients for each band, like the ones shown in Fig. 2. Here, the group velocity of the propagating beam is severely affected when additional FB modes are excited in various bands due to the low spatial coherence (see Fig. 4) of the incident beam. As a consequence, the number of modes belonging to the final superposition increases, changing substantially the correlations between the various modes. The consequence is that the averaged group velocity will not maintain periodic coherence during propagation.

IV. CONCLUSIONS

We have presented a theory of diffraction of partially coherent paraxial optical beams propagating through a

periodic medium. Within the framework of Floquet-Bloch waves, we have considered a linear combination of FB modes with random coefficients to obtain a general expression for the cross-spectral density $W(x_1, x_2, z)$ at propagation distance z . Considering as input a Gaussian-Schell beam, we have shown that weak correlations may modify severely the power distribution of the FB modes by spreading the power among additional FB wave vectors, in contrast with the fully coherent beam, whose FB power content is localized within a finite bandwidth in the neighborhood of the input wave vector. In an intermediate regime of coherence the modes tend to broaden up to the point of low coherence, where the power distribution is extended to all over the BZ and the beam profile can hardly note the grating.

A knowledge of the changes as light propagates through the transverse periodic medium in the presence, as well as in the absence, of field fluctuations is necessary to understand their influence upon light transport. These properties depend basically on the band structure. By introducing the statistical properties of the optical field in the investigation of beam propagation, one should unravel useful phenomena that will lead to remarkable techniques that manipulate light using the notion of coherence.

ACKNOWLEDGMENTS

The authors would like to thank the Brazilian Agencies FAPESP, CNPq, and CAPES for partial financial support. M.J.C. acknowledges fruitful discussions with J. C. A. Rocha throughout this work.

-
- [1] E. Yablonovitch, Inhibited Spontaneous Emission in Solid-State Physics and Electronics, *Phys. Rev. Lett.* **58**, 2059 (1987).
 - [2] S. John, Strong Localization of Photons in Certain Disordered Dielectric Superlattices, *Phys. Rev. Lett.* **58**, 2486 (1987).
 - [3] J. D. Joannopoulos, S. G. Johnson, J. N. Winn, and R. D. Meade, *Photonic Crystals Molding the Flow of Light* (Princeton Univ. Press, Princeton, 2008).
 - [4] P. S. J. Russell, Optics of Floquet-Bloch waves in dielectric gratings, *Appl. Phys. B* **39**, 231 (1986).
 - [5] K. Sakoda, *Optical Properties of Photonic Crystals*, 2nd ed., Optical Sciences (Springer, Heidelberg, 2005).
 - [6] P. Sheng, *Introduction to Wave Scattering, Localization, and Mesoscopic Phenomena*, 2nd ed. (Academic, San Diego, 2000).
 - [7] I. L. Garanovich, S. Longhi, A. A. Sukhorukov, and Y. S. Kivshar, Light propagation and localization in modulated photonic lattices and waveguides, *Phys. Rep.* **518**, 1 (2012).
 - [8] A. S. Ostrovsky, M. Á. Olvera-Santamaría, and P. C. Romero-Sorúa, Effect of coherence and polarization on resolution of optical imaging system, *Opt. Lett.* **36**, 1677 (2011).
 - [9] E. Baleine and A. Dogariu, Variable coherence tomography, *Opt. Lett.* **29**, 1233 (2004).
 - [10] A. Norrman, S. A. Ponomarenko, and A. T. Friberg, Partially coherent surface plasmon polaritons, *Europhys. Lett.* **116**, 64001 (2017).
 - [11] O. Korotkova and G. Gbur, Applications of optical coherence theory, *Prog. Opt.* **65**, 43 (2020).
 - [12] A. Nardi, S. Divitt, M. Rossi, F. Tebbenjohanns, A. Militaru, M. Frimmer, and L. Novotny, Encoding information in the mutual coherence of spatially separated light beams, *Opt. Lett.* **47**, 4588 (2022).
 - [13] E. Wolf and D. F. James, Correlation-induced spectral changes, *Rep. Prog. Phys.* **59**, 771 (1996).
 - [14] J. W. Goodman, *Statistical Optics* (Wiley, New York, 2015).
 - [15] E. Wolf, *Introduction to the Theory of Coherence and Polarization of Light* (Cambridge University, Cambridge, 2007).
 - [16] O. Korotkova, M. Salem, and E. Wolf, Beam conditions for radiation generated by an electromagnetic Gaussian Schell-model source, *Opt. Lett.* **29**, 1173 (2004).
 - [17] K. G. Makris, R. El-Ganainy, D. N. Christodoulides, and Z. H. Musslimani, Pt-symmetric optical lattices, *Phys. Rev. A* **81**, 063807 (2010).
 - [18] H. S. Eisenberg, Y. Silberberg, R. Morandotti, and J. S. Aitchison, Diffraction Management, *Phys. Rev. Lett.* **85**, 1863 (2000).
 - [19] J. J. Sakurai, *Advanced Quantum Mechanics* (Pearson, Delhi, 2006).
 - [20] V. S. Shchesnovich and S. Chávez-Cerda, Bragg-resonance-induced Rabi oscillations in photonic lattices, *Opt. Lett.* **32**, 1920 (2007).
 - [21] P. A. Brandão and S. B. Cavalcanti, Bragg-induced power oscillations in pt-symmetric periodic photonic structures, *Phys. Rev. A* **96**, 053841 (2017).

- [22] S. Longhi, Photonic analog of Zitterbewegung in binary waveguide arrays, *Opt. Lett.* **35**, 235 (2010).
- [23] H. Buljan, G. Bartal, O. Cohen, T. Schwartz, O. Manela, T. Carmon, M. Segev, J. Fleischer, and D. Christodoulides, Partially coherent waves in nonlinear periodic lattices, *Stud. Appl. Math.: Special issue: Nonlinear optics* **115**, 173 (2005).
- [24] B. J. Hoenders and M. Bertolotti, Theory of partial coherence for weakly periodic media, *J. Opt. Soc. Am. A* **22**, 2682 (2005).
- [25] P. A. Brandão and J. C. A. Rocha, Propagation of partially coherent light in non-Hermitian lattices, *Phys. Rev. A* **106**, 063503 (2022).
- [26] P. De Santis, F. Gori, G. Guattari, and C. Palma, An example of a Collett-Wolf source, *Opt. Commun.* **29**, 256 (1979).
- [27] Q. He, J. Turunen, and A. T. Friberg, Propagation and imaging experiments with Gaussian Schell-model beams, *Opt. Commun.* **67**, 245 (1988).